JOURNAL OF GEOPHYSICAL RESEARCH, VOL. 114, D23306, doi:10.1029/2009JD012166, 2009

Isotopic composition of waters from Ethiopia and Kenya: Insights into moisture sources for eastern Africa

Naomi E. Levin,[1,2] Edward J. Zipser,[3] and Thure E. Cerling[1]

Received 31 March 2009; revised 26 June 2009; accepted 3 September 2009; published 8 December 2009.

[1] Oxygen and deuterium isotopic values of meteoric waters from Ethiopia are unusually high when compared to waters from other high-elevation settings in Africa and worldwide. These high values are well documented; however, the climatic processes responsible for the isotopic anomalies in Ethiopian waters have not been thoroughly investigated. We use isotopic data from waters and remote data products to demonstrate how different moisture sources affect the distribution of stable isotopes in waters from eastern Africa. Oxygen and deuterium stable isotopic data from 349 surface and near-surface groundwaters indicate isotopic distinctions between waters in Ethiopia and Kenya and confirm the anomalous nature of Ethiopian waters. Remote data products from the Tropical Rainfall Measuring Mission (TRMM) and National Centers for Environmental Prediction (NCEP) reanalysis project show strong westerly and southwesterly components to low-level winds during precipitation events in western and central Ethiopia. This is in contrast to the easterly and southeasterly winds that bring rainfall to Kenya and southeastern Ethiopia. Large regions of high equivalent potential temperatures (θ_e) at low levels over the Sudd and the Congo Basin demonstrate the potential for these areas as sources of moisture and convective instability. The combination of wind direction data from Ethiopia and θ_e distribution in Africa indicates that transpired moisture from the Sudd and the Congo Basin is likely responsible for the high isotopic values of rainfall in Ethiopia.

Citation: Levin, N. E., E. J. Zipser, and T. E. Cerling (2009), Isotopic composition of waters from Ethiopia and Kenya: Insights into moisture sources for eastern Africa, *J. Geophys. Res.*, *114*, D23306, doi:10.1029/2009JD012166.

1. Introduction

[2] Stable isotopes of oxygen and hydrogen in precipitation can be used to track meteorological processes because the distribution of a heavy or light isotope in water depends on equilibrium and kinetic processes associated with water's phase transitions. In the tropics, rainfall amount, altitude, distance from coastlines, moisture source, and humidity are the dominant controls on oxygen and hydrogen isotopes in precipitation [*Dansgaard*, 1964; *Gedzelman and Lawrence*, 1990; *Lawrence et al.*, 2004; *Rozanski et al.*, 1993]. Rainfall in most of Ethiopia is a well-noted exception to these trends because its oxygen isotope composition is independent of rainfall amount, altitude, or distance from coastlines [*Dansgaard*, 1964; *Rozanski et al.*, 1996].

[3] A comparison between $\delta^{18}O$ values of rainfall in Addis Ababa, Ethiopia and Dar es Salaam, Tanzania demonstrates the anomalous nature of Ethiopian waters (Figure 1). Addis Ababa (latitude 9.00°N, longitude 38.73°E, 2360 m above sea level) is more than 500 km from the nearest coastline in the Gulf of Aden and more than 1000 km from the Indian Ocean. Dar es Salaam is a coastal city (latitude 6.88°S, longitude 39.20°E, 55 m above sea level), and the only station within the Global Network of Isotopes in Precipitation (GNIP) in eastern Africa that documents $\delta^{18}O$ values of precipitation that comes directly from the Indian Ocean [*Rozanski et al.*, 1996; International Atomic Energy Agency (IAEA), Global network of isotopes in precipitation, The GNIP Database, 2006, http://isohis.iaea.org]. Since these sites receive comparable amounts of precipitation annually, global trends would predict lower oxygen and hydrogen isotope ratios of precipitation in Addis Ababa than in Dar es Salaam, due to lower mean annual temperature in Addis Ababa and increased fractionation due to both the continental and altitude effects [*Rozanski et al.*, 1996]. However, rainfall isotope data from GNIP show the opposite trend. Oxygen isotope ratios of rainfall in Addis Ababa are higher than those in Dar es Salaam, except during the rainy season when they overlap (Figure 1).

[4] Several explanations have been proposed for the anomalous isotopic distributions in Ethiopian rainfall. *Dansgaard* [1964], who initially recognized that the stable isotope ratios of Ethiopian waters were unusual, suggested that partial evaporation of rainfall and reexchange with moisture near the ground could produce the high isotope

[1]Department of Geology and Geophysics, University of Utah, Salt Lake City, Utah, USA.
[2]Now at Department of Earth and Planetary Sciences, Johns Hopkins University, Baltimore, Maryland, USA.
[3]Department of Atmospheric Sciences, University of Utah, Salt Lake City, Utah, USA.

0148-0227/09/2009JD012166$09.00

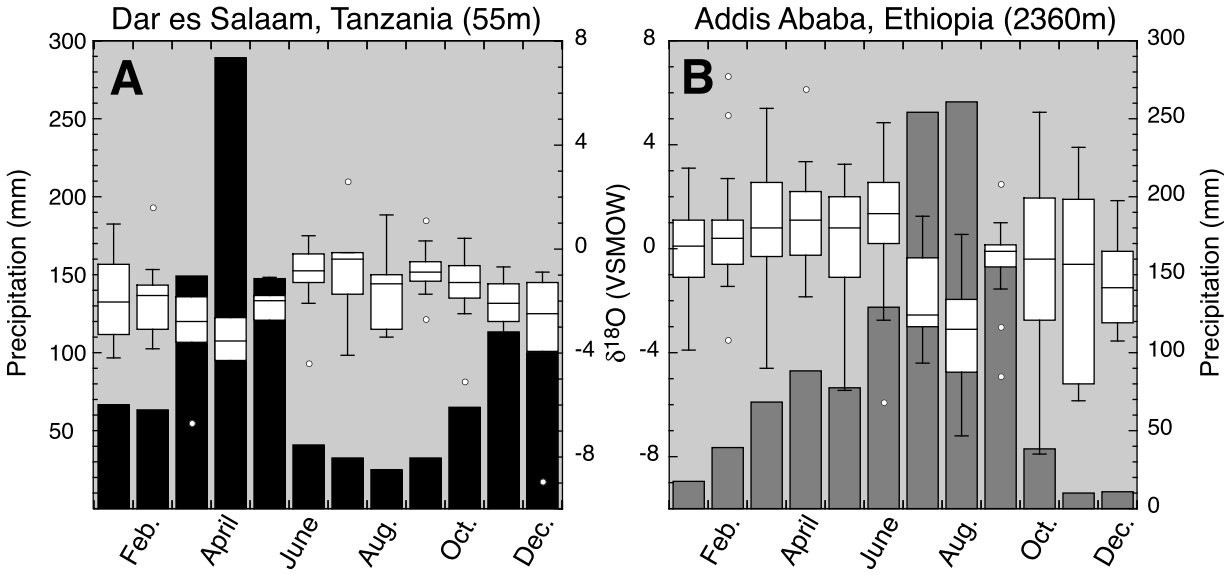

Figure 1. Box and whisker plots of GNIP monthly precipitation δ^{18}O values, in ‰ units, overlain on bars representing monthly rainfall accumulation for (a) Dar es Salaam (years 1960–1976) and (b) Addis Ababa (years 1961–2004). Adapted from *Rozanski et al.* [1996] using data from IAEA (Global network of isotopes in precipitation, The GNIP Database, 2006, http://isohis.iaea.org). The δ^{18}O values are not normalized to rainfall amount.

values. *Sonntag et al.* [1979] proposed that westerly, recycled moisture from the Congo Basin could explain high oxygen-18 and deuterium isotope concentrations in Ethiopian rainfall, because transpired moisture does not experience isotopic differentiation and often yields δ^{18}O and δD values that are equal or greater than the isotopic composition of water vapor over the ocean [*Gat and Matsui*, 1991; *Salati et al.*, 1979]. In contrast, *Joseph et al.* [1992] proposed that the relatively ^{18}O-enriched Ethiopian waters represent the first rainout from Indian Ocean moisture as it moves westward.

[5] To further explore these trends, additional data are needed to bolster the long-term record from Addis Ababa and the sparse data from GNIP stations elsewhere in eastern Africa. Surface waters and shallow groundwaters can be useful indicators of the average isotopic composition of rainfall when long-term data sets are not available [*Kendall and Coplen*, 2001]. Although the isotopic composition of surface and shallow groundwaters are not true proxies for the isotopic composition of rainfall, given variability in catchment size, transport time, season, and evaporative enrichment, they are useful indicators of the isotopic composition of precipitation in regions where long-term precipitation collections are not available [*Poage and Chamberlain*, 2001; *Rowley and Garzione*, 2007].

[6] We investigate explanations for high oxygen isotope ratios of Ethiopian rainfall in three steps. First, we present oxygen and hydrogen stable isotope ratios of rain and of surface and near-surface waters from Ethiopia and Kenya. These data extend the geographic range of the GNIP data set and are used to test whether isotopic trends of waters from Addis Ababa reflect the isotopic composition of waters from elsewhere in eastern Africa. Second, remote data products from the Tropical Rainfall Measuring Mission (TRMM) and the National Centers for Environmental Prediction (NCEP) are used to identify wind patterns, moisture sources and regions of convective instability for Ethiopia and Kenya during rain events and for mean seasonal conditions. Last, climatic and isotopic data are integrated and used to develop a working explanation for the distribution of rainfall δ^{18}O and δD values eastern Africa. We propose that the Congo Air Boundary serves as an isotopic divide and separates two distinct moisture sources in the region, the Indian Ocean and transpired continental moisture.

2. Background

2.1. Overview of Stable Isotopes in Precipitation

[7] *Dansgaard* [1964] described the primary influences on the isotopic composition of precipitation, which include temperature, latitude, evaporation, rainfall quantity, altitude, and distance from coastlines. Most isotopic variability at low latitudes correlates to the latter three factors, which are known as the amount, altitude and continental effects. These 'effects' are commonly attributed to Rayleigh fractionation, where condensation prefers the heavier nuclides and the remaining pool of vapor becomes depleted in the heavy isotope. As condensation of water continues throughout a storm, up a mountain, or across a continent, the remaining pool of vapor becomes progressively depleted in the heavy isotope, resulting in rainfall in coastal areas that is enriched in the heavy isotope relative to rainfall at inland or high elevation sites [*Dansgaard*, 1964; *Gat*, 2000]. Although the model of Rayleigh fractionation can describe general isotopic trends in the tropics, it does not account for in-cloud and storm-level isotopic processes, which are better explained by the physical controls on precipitation [e.g., *Gedzelman and Lawrence*, 1990; *Gedzelman and Arnold*, 1994; *Lawrence and White*, 1991; *Lawrence et al.*, 2004; *Risi et al.*, 2008].

[8] Evaporation plays an important role in the distribution of oxygen and hydrogen isotopes in rainfall. During evaporation, when vapor diffuses across the boundary layer, a

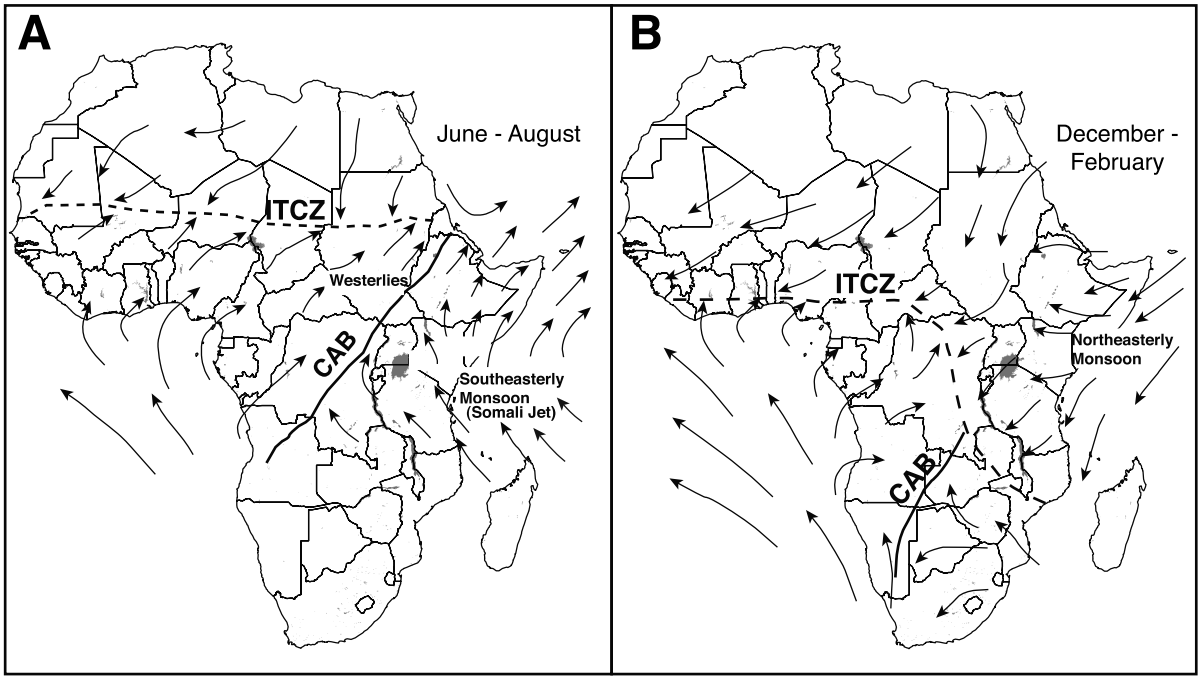

Figure 2. Schematics of low-level mean wind directions for tropical Africa in (a) the boreal summer (June–August) and (b) the austral summer (December–February), based on NCEP reanalysis 925 hPa mean winds and work by *Nicholson* [1996]. The approximate positions of the Intertropical Convergence Zone (ITCZ) and the Congo Air Boundary (CAB) are marked in addition to airstreams discussed in the text.

kinetic effect further depletes the resultant vapor of heavy isotopes relative to the remaining pool of water [*Craig and Gordon*, 1965]. The isotopic fractionation associated with this kinetic effect is amplified in conditions of low humidity.

[9] The isotopic composition of waters is commonly reported in δ notation and per mil (‰) units, where $\delta = ((R_{sample}/R_{standard}) - 1)*1000$ and R is the ratio of the heavy and light isotopes (e.g., $^{18}O/^{16}O$ and $^{2}H/^{1}H$). The isotope ratio of ocean water, Standard Mean Ocean Water (SMOW), is commonly used as a standard for calculating water δ values. The global meteoric water line (GMWL) is the linear relationship between oxygen ($\delta^{18}O$) and deuterium (δD) values of precipitation [*Dansgaard*, 1964]. Deviations from the GMWL are due to kinetic effects associated with evaporation [*Gat*, 1996; *Gonfiantini*, 1986]. Rainfall or water bodies that have experienced evaporative loss plot below and to the right of the GMWL, whereas the resultant water vapor plots above and to the left of the GMWL. Rain condensed from such vapor will plot on a line parallel to the GMWL but with a greater y intercept, or deuterium excess (where deuterium excess = $\delta D - 8*\delta^{18}O$). The deuterium excess, or d-excess, of precipitation reflects the degree of evaporation at the moisture source or the amount of evaporative enrichment in ^{18}O after water has condensed [*Gat et al.*, 1994; *Gat*, 1996].

[10] Although the ocean is the primary source for most rainfall, transpired moisture can be an important moisture source for many terrestrial regions [*Brubaker et al.*, 1993]. In regions with large amounts of evapotranspiration there is no net isotopic fractionation between a water source and the resultant vapor because all of the water consumed by plants is returned to the atmosphere. As a consequence of this wholesale return of water to the atmosphere, precipitation that originates from transpired moisture can yield $\delta^{18}O$ and δD values that are of equal or greater value than that of the initial ocean source water, but with an unchanged d-excess [*Gat and Matsui*, 1991; *Moreira et al.*, 1997; *Salati et al.*, 1979; *Worden et al.*, 2007]. The effects of transpiration are best documented in the Amazon, where rainfall produced from transpired moisture plots directly on the meteoric water line (d-excess $\approx$ 10‰), making it distinct from rainfall that originates from evaporated moisture, which has higher d-excess values [*Gat and Matsui*, 1991; *Moreira et al.*, 1997; *Victoria et al.*, 1991]. These studies demonstrate that stable isotopes can be used to identify precipitation recycled by transpiration because (1) the lack of isotopic differentiation makes it distinct from precipitation that is depleted in heavy isotopes due to Rayleigh fractionation processes and (2) relatively low d-excess values make precipitation recycled through transpiration isotopically distinct from precipitation that has been recycled via evaporation from soil or surface waters.

2.2. Climate in Eastern Africa

[11] Equatorial eastern Africa is considered one of the more meteorologically complex parts of Africa [*Nicholson*, 1996]. The main factors influencing rainfall in eastern Africa are low-level air streams, convergence zones between these air streams, and topography. The three major air streams for eastern Africa are (1) the northeast monsoon that brings predominantly dry air, (2) the southeast monsoon system from the Indian Ocean, and (3) westerly southwesterly humid Congo air [*Nicholson*, 1996]. The Intertropical Convergence Zone (ITCZ) separates the northeast and southeast monsoons, whereas the Congo Air Boundary separates westerly flow from easterly low-level flows (Figure 2).

The timing and strength of these two monsoon systems control the seasonal distribution of rainfall in eastern Africa. The two rainy seasons in Kenya include the Masika rains in March through May and the Vuli rains in October through December, which are shorter in seasonal duration and less intense than the Masika rains [*Camberlin and Philippon*, 2002]. Precipitation during both seasons is brought by southeasterly winds from the Indian Ocean [*Griffiths*, 1972; *Nicholson*, 1996]. In Ethiopia, the 'big rains', or Kiremt, last from June through September and are sourced by moist southwesterlies and westerlies, whereas the Belg is the shorter rainy season, which occurs during March through May and is associated with the southeastern monsoon [*Gamachu*, 1977; *Griffiths*, 1972; *Vizy and Cook*, 2003]. The Belg rains lose their influence in northern Ethiopia, where there is only one annual peak of rainfall that lasts between June and September. However, in southeastern Ethiopia, rainfall is evenly distributed between the two rainy seasons in March–May and in July–October [*Gamachu*, 1977]. The timing and extent of rainy seasons vary with latitude and topography in both countries [*Gamachu*, 1977; *Nicholson*, 1996].

[12] The high plateaus (1000–1500 m), mountains (>4000 m), and varied topography in Kenya and Ethiopia affect regional climate by channeling or blocking low-level airstreams, orographic lifting of air masses, convective heating, and rain shadow effects. The highlands have a critical influence on the Somali Jet, which is part of the southeasterly monsoon system that moves into Kenya from the Indian Ocean, travels northward, and curves northeast toward Somalia and the Arabian Sea, becoming the southwest monsoon of the Indian subcontinent (Figure 2). At the equator the Kenyan highlands block the Somali Jet from penetrating further west and the Ethiopian highlands are the Jet's northern limit before it moves eastward again [*Krishnamurti et al.*, 1976; *Slingo et al.*, 2005] (Figure 2). The highlands also block moist westerly air from reaching the eastern portions of Ethiopia and Kenya.

2.3. Remote Data Products

[13] The TRMM satellite was launched in 1998. It is equipped with the first Precipitation Radar (PR) in space, a passive Microwave Imager (TMI), a Visible and Infrared Scanner (VIRS), and a Lightning Imaging Sensor (LIS) [*Kummerow et al.*, 1998]. This suite of instruments facilitates many types of studies, including estimating precipitation amount and area, convective activity, diurnal cycles and storm structure [*Kummerow et al.*, 1998; *Liu and Zipser*, 2008; *Nesbitt and Zipser*, 2003; *Schumacher and Houze*, 2006]. The PR on TRMM is a 13.8 GHz radar with a swath 220 km wide and visits a location on average once every 2–3 days near the equator [*Kozu et al.*, 2001; *Kummerow et al.*, 1998; *Negri et al.*, 2002]. The horizontal resolution is 4.2 km before August 2001 and 5 km after August 2001 [*Wilcox and Ramanathan*, 2001]. The satellite's non-Sun-synchronous orbit enables sampling of the full diurnal cycle.

[14] Ground validation studies show high correlations ($r^2 > 0.9$) between PR rainfall estimates and those from gauge-calibrated ground radar [*Anagnostou and Morales*, 2002; *Liao et al.*, 2001]. Rainfall estimates from remote methods, like those produced by TRMM, can be useful in places like Africa where ground-based data are limited. In Africa, comparisons with gauge data show that the TRMM PR overestimates rainfall amount, especially when and where rainfall is low, whereas the TRMM-merged rainfall products, which include an additional suite of remote data products, show excellent agreement with gauge data [*Adeyewa and Nakamura*, 2003; *Dinku et al.*, 2007; *Nicholson et al.*, 2003].

[15] Data from the TRMM satellite have been used to identify Radar Precipitation Features (RPFs), which are defined as a group of contiguous pixels that indicate near-surface rainfall based on a suite of TRMM data attributes [*Liu et al.*, 2008; *Nesbitt et al.*, 2000]. The size of a RPF is indicative of storm size and is related to rain volume. In the tropics, most large storms are mesoscale convective systems (MCSs), which are defined by *Houze* [1993] as "cloud system[s] that occurs in connection with an ensemble of thunderstorms and produces a contiguous precipitation area ~100 km or more in horizontal scale in at least one direction." MCSs are identified in the TRMM data set as RPFs with area >2000 km^2 [*Liu et al.*, 2008; *Nesbitt et al.*, 2000].

[16] The National Centers for Environmental Prediction (NCEP) and National Center for Atmospheric Research (NCAR) have cooperated in compiling and analyzing more than 50 years of atmospheric data, including data from the land surface, ship, rawinsonde, aircraft and satellite [*Kalnay et al.*, 1996; *Kistler et al.*, 2001]. The reanalysis uses a numerical simulation model that is continuously updated by data assimilation to produce a three-dimensional global data set of atmospheric parameters over a $2.5° \times 2.5°$ grid. The NCEP/NCAR reanalysis database integrates atmospheric data from the available data sources and provides a useful tool for investigating climate [e.g., *Vizy and Cook*, 2003].

3. Materials and Methods

3.1. Stable Isotope Ratio Measurements

[17] Stream, river, spring, well, rain and tap water samples (n = 349) were collected in Kenya and Ethiopia between 1975 and 2007. The majority of the sampling sites are concentrated in the rift valley and highland regions of both countries. These sites are binned into zones to evaluate geographic variability in isotopic and climate data (Figure 3). Waters were collected in 1 dram glass vials with Teflon coated rubber septa (rubber side facing sample) and others in Qorpak® vials with polycone seal caps. Data from geothermal waters, lakes and pools were excluded from this study.

[18] Oxygen and hydrogen isotope ratios of waters were determined using manual and automated methods. The majority of measurements were made at the University of Utah, except as noted below. Hydrogen isotope ratios were determined by analysis of H_2 gas produced by reduction of 2 μl water sample with Zn reagent at 500°C [*Coleman et al.*, 1982] and measured on a Finnigan Delta S mass spectrometer. Oxygen isotope ratios were determined by measurement of CO_2 gas equilibrated with 500 μl to 5 ml of sample water at 25°C for 48 h and measured either by dual inlet or continuous flow mode of a Finnigan mass spectrometer, using methods adapted from *Epstein et al.* [1953] and *Fessenden et al.* [2002]. Precision of internal standards used for the offline measurements was 0.2‰ and 1.5‰ for $\delta^{18}O$ and δD, respectively. Automated analyses of

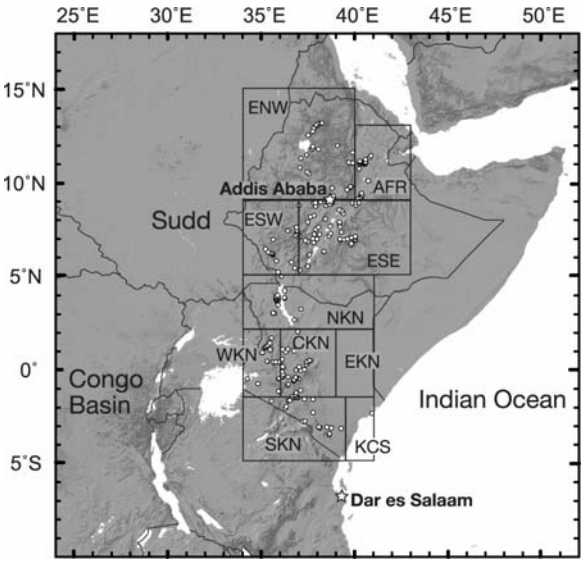

Figure 3. Location of water sampling sites marked with dots, overlain on a Shuttle Radar Topography Mission digital elevation model. The locations of GNIP collections sites discussed in the text are marked with stars. Geographic zones used to examine data are outlined and abbreviated as northwestern Ethiopia (ENW), Afar (AFR), southwestern Ethiopia (ESW), southeastern Ethiopia (ESE), northern Kenya (NKN), western Kenya (WKN), central Kenya (CKN), eastern Kenya (EKN), southern Kenya (SKN), and coastal Kenya (KCS).

waters were performed using a single 0.5 μl aliquot of water injected onto a glassy carbon column that was held at 1400°C to produce H_2 and CO_2 gases [*Sharp et al.*, 2001]. After separation by a gas chromatograph in a helium carrier gas, the isotope ratios of these gases were analyzed with a ThermoFinnigan Delta +XL mass spectrometer. Samples were measured in duplicate with an average precision (1σ) of 0.2‰ and 1.3‰ for $\delta^{18}O$ and δD, respectively. Some $\delta^{18}O$ and δD data from Ethiopian waters (n = 18), that were previously published by *Levin et al.* [2004] and analyzed at the University of Arizona, are also included in the water isotope data set presented and discussed here. Likewise, previously published data from Kenya (n = 5) are also included here [*Barton et al.*, 1987]. Oxygen and hydrogen isotopic ratios are reported in δ notation in reference to the isotope standard VSMOW (Vienna Standard Mean Ocean Water). Where reported below, the error on a statistic represents the standard deviation.

3.2. Remote Data

[19] TRMM Precipitation Radar (PR version 6, 2A25) data from the 1998–2007 collection period were used to identify Radar Precipitation Features (RPFs) as defined by *Liu et al.* [2008]. The 2.5° latitude × 2.5° longitude NCEP/NCAR reanalysis data set from six hour intervals [*Kalnay et al.*, 1996] was used to identify wind direction during specific RPFs and average seasonal conditions. NCEP/NCAR wind direction data for specific times and locations were generated by temporal interpolation and spatially from the nearest neighbor, based on methods used by *Liu et al.* [2008]. Wind angles were generated from NCEP/NCAR reanalysis sounding data for times and location of mesoscale convective systems (MCSs) events at the 850 hPa level, roughly equivalent to 1500 m above sea level. Data retrieval was focused at the 850 hPa level, which is high enough to minimize the effects of topographic interference but low enough to characterize conditions in the lower troposphere outside the highlands. Where the land surface lies above 1500 m, the reanalysis data at 850 hPa is an unjustifiable extrapolation to levels that are beneath the surface. Despite these well-known difficulties in regions of complex terrain, this is deemed a better approximation to near-surface conditions than the next available standard level of more than 3000 m above sea level.

[20] Equivalent potential temperature (θ_e) is the temperature reached if an air parcel is lifted adiabatically until all of its water has condensed and then adiabatically descends to a pressure of 1000 hPa. The θ_e is used as an indicator of atmospheric instability in the lower atmosphere (>800 hPa). High θ_e at low levels is a necessary condition for deep convection because it indicates a moist air parcel with temperatures warm enough to make it potentially buoyant with respect to its surrounding environment, through release of latent heat of condensation. The majority of rainfall in tropical Africa is convective [*Zipser et al.*, 2006] and must originate from regions with relatively high θ_e. Here, θ_e is used to identify moisture sources for rainfall in Kenya and Ethiopia.

4. Results

4.1. Isotopic Composition of Waters

[21] The $\delta^{18}O$ and δD values of precipitation, surface, and near-surface waters are plotted in reference to the GWML, the local MWL established for Addis Ababa (AddMWL), and an average of MWLs for Africa (AfrMWL) [*Cohen et al.*, 1997; *Rozanski et al.*, 1996] (Figure 4).

[22] The $\delta^{18}O$ and δD values of waters from Kenya and Ethiopia are distinct (Figure 4 and auxiliary material[1] Data Set S1). The $\delta^{18}O$ values from Kenya waters average -2.5 ± 2.4‰ (n = 181), whereas Ethiopian waters yield $\delta^{18}O$ values that average -0.2 ± 1.8‰ (n = 165). $\delta^{18}O$ values of waters from Ethiopia are significantly higher than those from Kenya (separate variance t test $p < 0.0001$). However, the d-excess values from Kenyan waters (average 11.2 ± 9.2‰; n = 149) are significantly higher than those from Ethiopia (average 6.5 ± 5.7‰; n = 164) (separate variance t test, $p < 0.001$). Within this data set there are no significant differences in $\delta^{18}O$ or δD values of waters sampled from different zones within Kenya or Ethiopia.

[23] There are no significant trends between elevation and $\delta^{18}O$ values of waters from Ethiopia and Kenya (Figure 5). The varying effects of evaporative enrichment on waters from similar elevations may be responsible for the lack of significant altitude effects. The influence of evaporation can be reduced by limiting the sample to waters that plot within ±2‰ of the d-excess expected for the GMWL, AddMWL, and AfrMWL. Among these waters there are weak ($r^2 > 0.5$)

[1] Auxiliary materials are available at ftp://ftp.agu.org/apend/jd/2009jd012166.

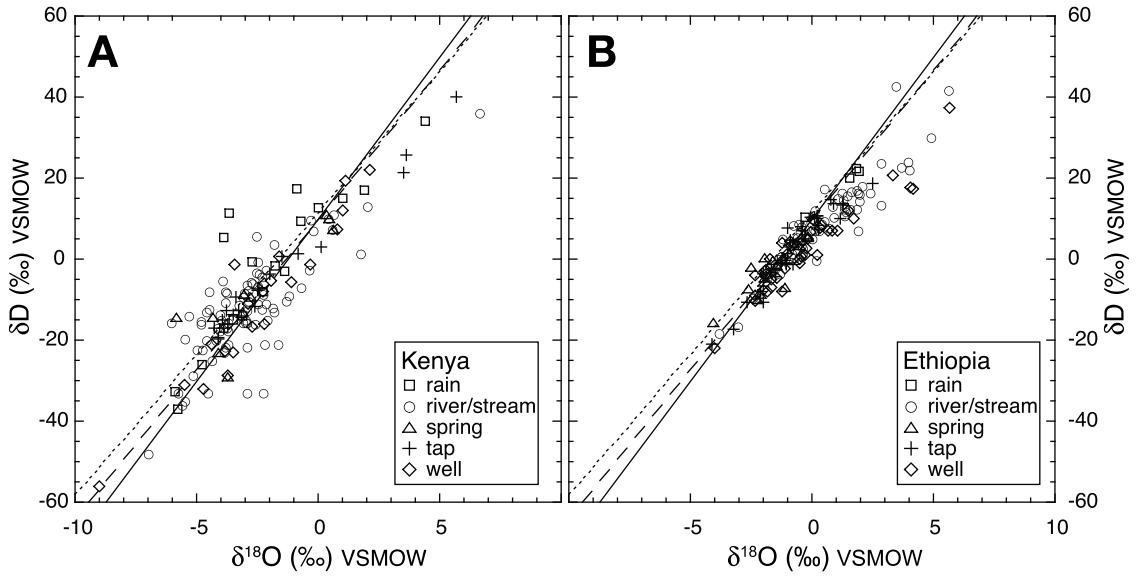

Figure 4. Oxygen and hydrogen isotope ratios of rain, river, spring, tap, and well waters from (a) Kenya and (b) Ethiopia. The global (solid line: $\delta D = 8*\delta^{18}O + 10$), Addis Ababa (dotted line: $\delta D = 6.95 \pm 0.22*\delta^{18}O + 11.51 \pm 0.58$), and Africa meteoric water lines (dashed line: $\delta D = 7.4*\delta^{18}O + 10.1$) are plotted for reference [*Dansgaard*, 1964; *Rozanski et al.*, 1996; *Cohen et al.*, 1997].

linear $\delta^{18}O$ altitude trends for southern Kenya, southeast Ethiopia and southwest Ethiopia, but there are no significant trends for the other regions (Figure 5). The slopes for these trends indicate a 0.5–1.3‰ decrease in $\delta^{18}O$ value for every kilometer increase in elevation.

4.1.1. Isotopic Distinctions Between Ethiopian and Kenyan Waters

[24] The contrast in $\delta^{18}O$ and δD values between Ethiopian and Kenyan surface and subsurface waters confirms previous observations that Ethiopian waters have higher $\delta^{18}O$ values than other waters from eastern Africa at similar altitudes. In Ethiopia, where many regions are characterized by low relative humidity, it would be reasonable to view the evaporative enrichment of raindrops as a primary cause of the high isotopic values, as suggested by *Dansgaard* [1964]. However, most of these waters plot on the local and global MWLs, eliminating evaporated rainfall as a viable explanation. Instead, an explanation for the anomalous waters must lie in an ^{18}O-enriched moisture source and in phenomena that minimize the depletion of heavy isotopes normally associated with high-elevation, inland locations.

[25] Low d-excess values of waters from Ethiopia indicate enrichment in ^{18}O due to evaporation, as expected for river and shallow well waters in arid regions, like Afar, Ethiopia and northern Kenya (Figure 4). The prevalence of high d-excess values among Kenya waters may be indicative of precipitation that formed from water vapor evaporated near the land surface, either as a product of evaporated rainfall that recondenses or evaporation from surface waters, such as rift valley lakes [*Russell and Johnson*, 2006].

4.1.2. Altitude Effect

[26] Surface and near-surface waters are integrators of seasonal or annual precipitation and provide a useful perspective on the altitude effect in Ethiopia. The ^{18}O altitude trends observed for the Kenya and Ethiopian waters (-1.3‰ km^{-1} and -0.5‰ km^{-1}) are less pronounced than those observed elsewhere in the tropics, where ^{18}O altitude gradients vary between -2.7 ± 0.3‰ km^{-1} and -1.5 ± 0.3‰ km^{-1} [*Gonfiantini et al.*, 2001; *Lachniet and Patterson*, 2002].

[27] Although $\delta^{18}O$ altitude trends are not observed in every region sampled in this study, the presence of $\delta^{18}O$ altitude relationships in some regions suggests a muted altitude effect. If the altitude effect exists in eastern Africa with a smaller gradient, it will be difficult to detect this subtle trend using the data that are presently available from surface and subsurface water samples and widely dispersed precipitation records. Instead, more systematic collections of rainfall along elevation transects must be made for eastern Africa, like those of *Gonfiantini et al.* [2001].

4.2. Rainfall Climatology

[28] In this section, TRMM and NCEP/NCAR data products are used to evaluate climatic patterns and moisture sources that could influence the isotopic composition of precipitation from Ethiopia and Kenya.

[29] The distribution of MCSs (RPFs > 2000 km^2) mimics the seasonal distribution of rainfall in eastern Africa (Figure 6), marking patterns of two rainy seasons – the Kiremt (June–September) and Belg (March–May) in Ethiopia and the Masika (March–May) and Vuli rains (October–December) in Kenya. There is a notable absence of MCSs in southeastern Ethiopia during JJA when the Kiremt dominates the rest of Ethiopia. Instead, rainfall in southeastern Ethiopia is more similar to the rainy seasons in Kenya during MAM and SON.

[30] At the 850 hPa level, wind angle at the time of MCSs and RPFs varies by season and region. In Kenya, 850 hPa wind angle is southeasterly during the Masika and easterly during the Vuli rains (Figures 6 and 7). During the Kiremt (JJA) in Ethiopia, winds associated with rain events are westerly and southwesterly in central and northern Ethiopia, whereas they are easterly and southwesterly during the shorter Belg rains (MAM). In the southern parts of Ethiopia,

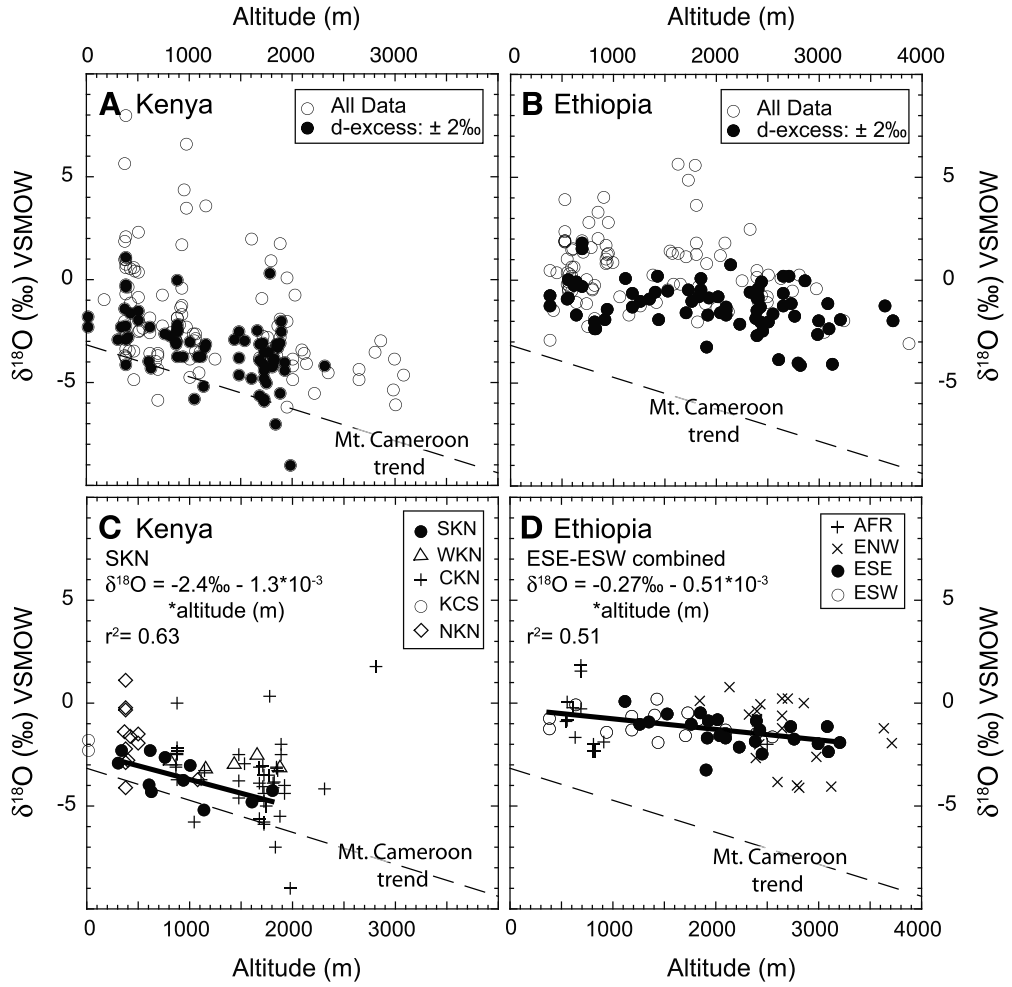

Figure 5. The $\delta^{18}O$ values of waters plotted versus altitude. All water data from (a) Kenya and (b) Ethiopia are plotted as open circles. Waters with a d-excess ±2‰ of expected from the MWLs (global, Addis Ababa, and Africa) are plotted as closed circles. The altitude $\delta^{18}O$ trends are plotted by region for (c) Kenya and (d) Ethiopia. Linear regressions ($r^2 > 0.5$) are plotted and the regression equations are listed. The altitude $\delta^{18}O$ regression for Mt. Cameroon from *Gonfiantini et al.* [2001] is plotted for reference in all plots. Abbreviations for regions in eastern Africa are the same as defined for Figure 3.

where large storms events are more common in MAM and SON, winds are southerly.

[31] The 850 hPa wind angles at the times and locations of individual MCS events are compromised by the high elevation of the land surface, as indicated in section 3.2, and by the uncertainty of the reanalysis in data sparse regions of complex terrain. Although these results give a consistent picture, the moisture source for the rain-producing storms may be more reliably indicated by the mean seasonal conditions. Contours of mean seasonal θ_e at 850 hPa are plotted with mean seasonal wind vectors (Figure 8). Mean seasonal wind vectors at 850 hPa confirm wind angle trends observed for individual MCSs and RPFs (Figures 6 and 7). Contours of θ_e follow regions of atmospheric instability, with high θ_e indicating regions that contain enough moisture and energy for convective activity. Ridges of high θ_e in southern Africa during the boreal winter (DJF) move to the north in the boreal summer (JJA) and track rainfall. During Ethiopia's Kiremt rains in JJA, 850 hPa mean wind vectors are southwesterly and southerly in the Ethiopian highlands, with regions of high θ_e to the west in central Africa and to the east on the Arabian Peninsula (Figure 8b), indicating air with high moisture content and convective instability. During this same season, wind vectors over the Indian Ocean are very strong and pull low θ_e air over Kenya, which is low in moisture content and a poor energy source for storms. These southeasterly winds are deflected by the southern Ethiopian highlands and do not penetrate further into Ethiopia. During the Masika rains (MAM), southeasterly winds bring moisture from the Indian Ocean into Kenya. Seasonal mean wind vectors indicate that some of this moisture reaches parts of Ethiopia, coinciding with the short rains and consistent with the wind directions for this region in MAM (Figures 6 and 7).

[32] The combination of θ_e and wind angle data suggests that there are two main moisture sources for eastern Africa, 1) marine vapor from the Indian Ocean and 2) terrestrial moisture from the Sudd and the Congo Basin. Strong southeasterly low-level winds moving from the Indian Ocean into Kenya and southern Ethiopia are coincident with elevated θ_e over the Indian Ocean in MAM. This combination of θ_e and low-level winds demonstrates the

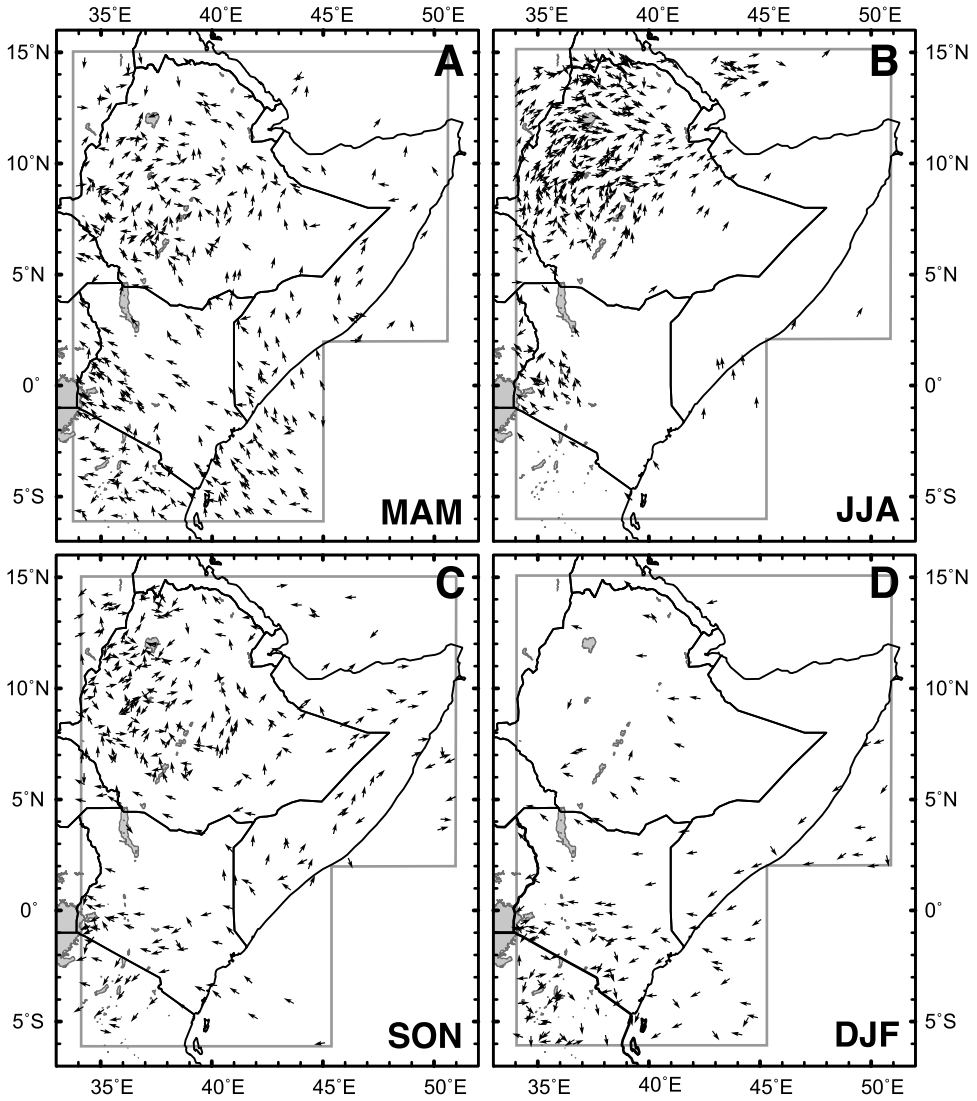

Figure 6. NCEP-derived 850 hPa wind angle for the time and location of mesoscale convective system (MCS) events identified for 1998–2000. Data are grouped by season: (a) March–May (MAM), (b) June–August (JJA), (c) September–November (SON), and (d) December–February (DJF). The gray outline on each map indicates the search area for MCS events.

Indian Ocean as a moisture source for precipitation during the southeast monsoon, which is a well-established pattern [*Nicholson*, 1996]. In JJA, when central and northern Ethiopia receives the majority of its rainfall, westerly and southwesterly low-level winds draw air from a region of high θ_e in southern Sudan and the northeastern Congo Basin. The combination of westerly southwesterly winds and θ_e contours suggest that recycled moisture from terrestrial sources fuels the rains during the boreal summer in all areas of Ethiopia except for the southern portion of the country.

[33] The role of transpired and recycled moisture on African climate is exemplified by θ_e contours at 925 hPa (Figure 9). Regions of high θ_e are constrained by the outline of the African continent and are centered in the Congo Basin for the majority of the year, where there is a large rain forest. In JJA, during the Kiremt rains in Ethiopia, regions of high θ_e at low levels are shifted northward toward the Sudd, an extensive region of swamps associated with the upper Nile River Basin. The restriction of high θ_e to terrestrial regions indicates that thermal instability and convective potential in Africa is associated with moisture content over land. *Hodges and Thorncroft* [1997] attributed this θ_e distribution to the moist lowlands of the Congo and the importance of fluxes from land surfaces as sources for convection rather than the ocean. Although low-level 925 hPa plots of θ_e (Figure 9) are useful to identify terrestrial moisture content over the Sudd and the Congo, and the low level airflow bringing this air toward Ethiopia, it is of limited use where the land surface is at higher elevations. The apparent high θ_e in the Ethiopian highlands year round (Figure 9) is an artifact of this incongruence and probably not commensurate with the true θ_e distribution in these high-elevation settings.

[34] The westerly and southwesterly flow of air and advection of moisture from the African interior into Ethiopia during the boreal summer has been noted in other studies [*Camberlin*, 1997; *Conway*, 2000; *Gamachu*, 1977; *Leroux*, 2001; *Slingo et al.*, 2005; *Vizy and Cook*,

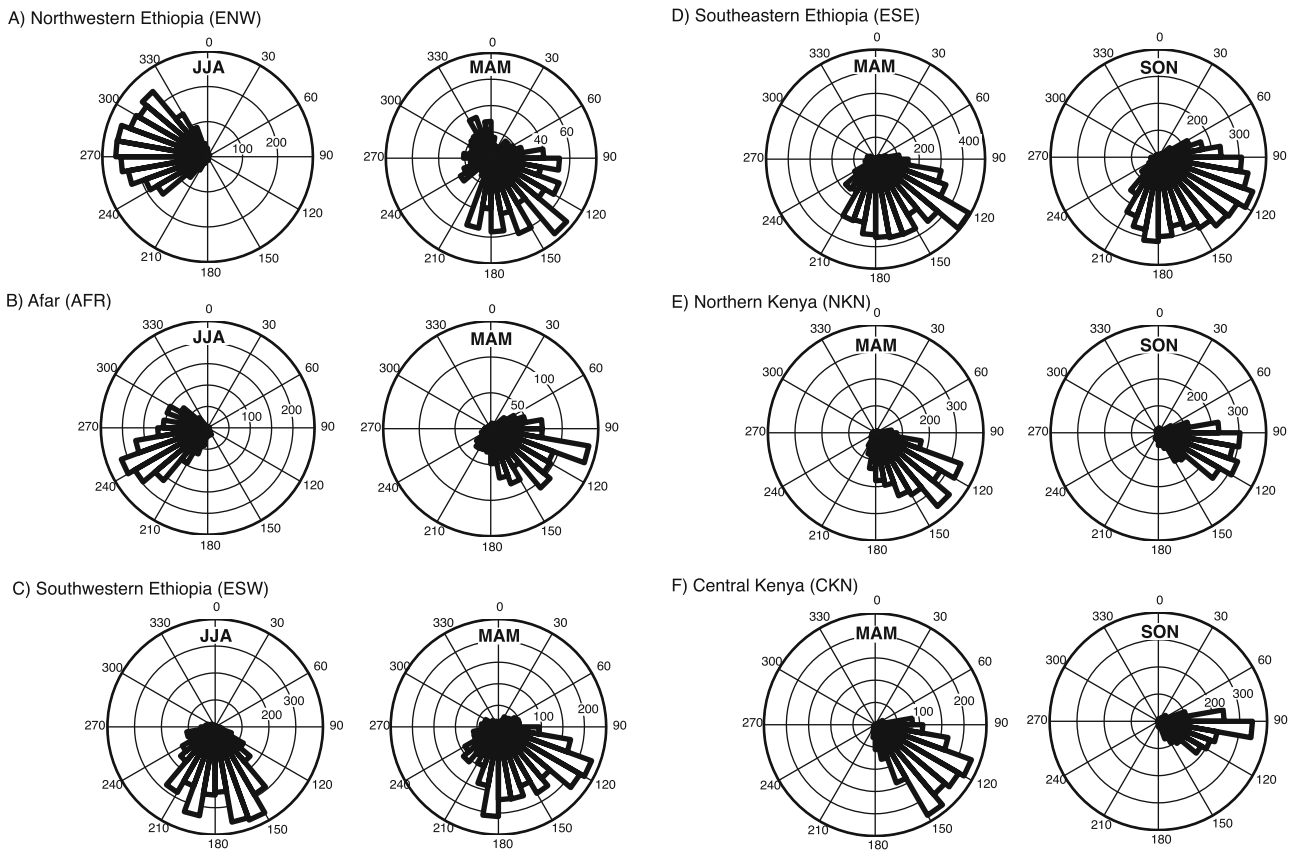

Figure 7. Histograms of wind angles during radar precipitation features (RPFs) at 850 hPa for the years 1998–2007. Data are plotted for the two seasons with the most number of RPFs in each region and include (a) northwestern Ethiopia, (b) Afar, (c) southwestern Ethiopia, (d) southeastern Ethiopia, (e) northern Kenya, and (f) central Kenya.

2003]. *Slingo et al.* [2005] performed numerical experiments with and without the Ethiopian highlands that implicated topography in blocking flow from the Indian Ocean and in permitting the air moistened over the Sudd and the Congo to reach the highlands instead. They also used a different reanalysis (from the European Centre for Medium-Range Weather Forecasting) to show that moist low-level airflow reaches Ethiopia from the southwest and west and that the highlands block westerlies from southern Ethiopia.

5. Discussion

[35] Precipitation in Kenya is fed by southeasterly winds, which bring moisture from the Indian Ocean. δ^{18}O values of waters sampled in Kenya are consistent with δ^{18}O values of the first rains from Indian Ocean moisture. Although the δ^{18}O altitude trend is muted, it is similar to that observed elsewhere in the tropics. The y intercept of the δ^{18}O altitude regression for the southern Kenya regression is similar to the δ^{18}O value of rainfall from coastal Kenya (Figure 5). The high d-excess of some waters from Kenya could be associated with condensation of vapor derived from partially evaporated raindrops. This is consistent with the low humidity characteristic of the rift valley setting where the majority of the waters were sampled. Rainfall in Ethiopia that is associated with southeasterly winds and sourced by Indian Ocean moisture should yield δ^{18}O values similar to δ^{18}O values of Kenyan rainfall. Any westerly or southwesterly moisture should have a different isotopic composition. The absence of these isotopic distinctions within Ethiopia may be a product of the uneven geographic distribution of the sampled waters.

[36] Westerlies and southwesterlies are responsible for precipitation in Ethiopia during the Kiremt (Figures 6 and 7). Vapor sources from the Sudd and in the Congo Basin are likely products of terrestrial water recycling, as demonstrated by the association of high θ_e with the continental outline in the lower troposphere (Figure 9). This pattern of high θ_e has been observed in other studies that demonstrate the importance of recycled moisture in tropical Africa [*Brubaker et al.*, 1993; *Gong and Eltahir*, 1996; *Trenberth*, 1999].

[37] The δ^{18}O and δD values of water formed from recycled moisture provide information about how that moisture was recycled in the source area. As discussed earlier, terrestrial water that is returned to the atmosphere through transpiration experiences no fractionation, producing water vapor that is enriched in ^{18}O relative to its source water but that plots on the local meteoric water line. In contrast, terrestrial water returned to the atmosphere through evaporation does fractionate, such that rainfall produced from evaporated sources has a high d-excess and is depleted in ^{18}O relative to the source water. The isotopic distinction between transpired and evaporated recycled water has been demonstrated in the Amazon and used as a tool for

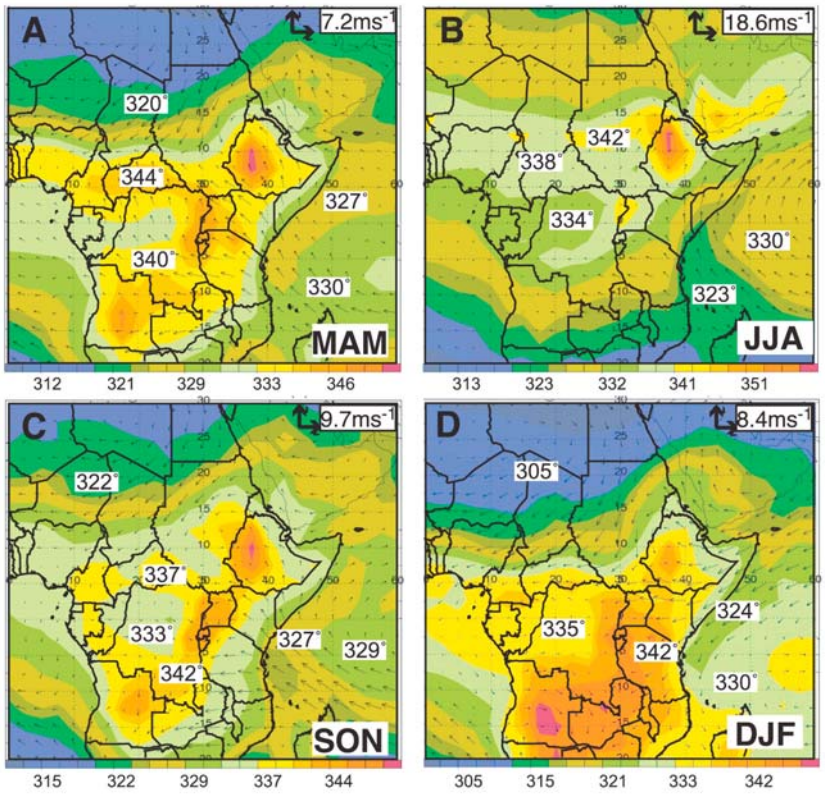

Figure 8. NCEP mean seasonal wind vectors and contours of θ_e at 850 hPa. Note that the scales for vectors and θ_e are different in the plots for each season. The θ_e temperatures are reported in degrees Kelvin. Color scales for θ_e are defined at the base of each plot, and vector scales are defined in the top right-hand corner of each plot. Plots were generated from: http://www.met.utah.edu/zipser/pub/projects/ncep/.

evaluating the terrestrial water cycle [*Gat and Matsui*, 1991; *Moreira et al.*, 1997; *Salati et al.*, 1979; *Victoria et al.*, 1991].

[38] If similar principles are applied, isotopic data from this study suggest that the recycled water source for Ethiopian rainfall likely has a significant transpired component because: (1) the d-excess of the waters are relatively low and are rarely greater than the local and global meteoric water lines, and (2) precipitation in Ethiopia is enriched in ^{18}O, not depleted in ^{18}O, as it would be if evaporated waters were the dominant moisture source. The importance of transpired moisture in controlling the isotopic composition of African precipitation has been suggested by *Taupin et al.* [2000], who note the absence of the continental effect in western Africa and suggest that the moisture is not fractionated but instead recycled through transpiration. Hydrological studies of the Sudd and Congo Basin typically group water loss from evaporation and transpiration into a single term [*Crowley et al.*, 2006; *Mohamed et al.*, 2006]. Separating these terms and evaluating their relative contribution to recycled moisture will be necessary for testing the role of transpired moisture on the isotopic composition of Ethiopian rainfall.

[39] Given the wind angle and θ_e data, recycled ^{18}O-enriched moisture from southern Sudan or the Congo is a likely candidate for the high $\delta^{18}O$ values of Ethiopian rainfall. Unfortunately, there are very few $\delta^{18}O$ and δD data from these regions. The GNIP station at Kinshasa, which is in the westernmost part of the Congo Basin and near the Atlantic coast, is not representative of the isotopic composition of water from the interior of the Congo Basin. Nor should the GNIP isotope data from Entebbe, Uganda be considered a useful gauge of water isotopes near the Congo because it is affected by moisture evaporated from Lake Victoria [*Rozanski et al.*, 1996]. We are not aware of isotopic data on waters from the Sudd, however there are published data that include water samples from springs, rivers, and isolated rain events in northeastern Congo and from western Uganda [*Cerling et al.*, 2004; *Russell and Johnson*, 2006; IAEA, Global network of isotopes in precipitation, The GNIP Database, 2006, http://isohis.iaea.org]. In general, these waters plot on or near the GMWL and the AfrMWL and range from −5.2‰ to +2.9‰. *Russell and Johnson* [2006] suggest that the high $\delta^{18}O$ values in rain and river waters originate from recycled and ^{18}O-enriched waters from the Congo Basin. Although there is only indirect evidence for the isotopic composition of Congo Basin moisture, the existing data suggest that this moisture could be one of the sources for the ^{18}O-enriched waters in Ethiopia.

[40] The Congo Air Boundary, which forms a midline in Africa and separates westerly and easterly low-level flow (Figure 2), could be considered an isotopic divide that separates the influence of relatively ^{18}O-depleted moisture from the Indian Ocean and recycled ^{18}O-enriched moisture from the African interior. If individual storms in Ethiopia were monitored for their isotopic composition, it is likely

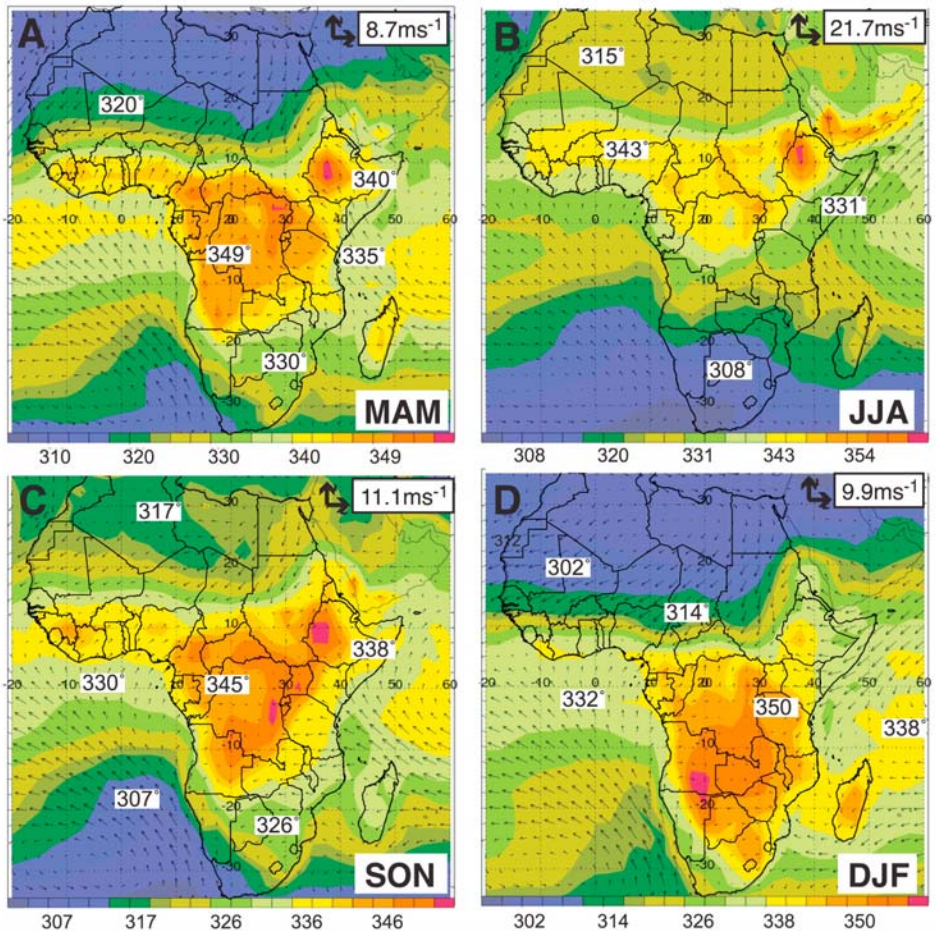

Figure 9. NCEP mean seasonal wind vectors and contours of θ_e at 925 hPa. Note that the scales for vectors and θ_e are different in the plots for each season. The θ_e temperatures are reported in degrees Kelvin. Color scales for θ_e are defined at the base of each plot, and vector scales are defined in the top right-hand corner of each plot. Plots were generated from: http://www.met.utah.edu/zipser/pub/projects/ncep/.

that storms associated with westerlies in JJA would yield precipitation with higher $\delta^{18}O$ values than storms associated with southeasterlies, which predominate in MAM. $\delta^{18}O$ values from precipitation associated with the MAM storms should more closely resemble the isotopic composition of rainfall in Kenya, which is also associated with southeasterlies that transport moisture from the Indian Ocean.

6. Conclusions

[41] Isotopic analysis of surface and subsurface waters from Ethiopia and Kenya confirms previous studies that indicate higher $\delta^{18}O$ values in waters from Ethiopia relative to waters from regions of similar elevation in tropical Africa. This study takes advantage of the relative ease of sampling surface and subsurface waters over a broad geographic area compared to the prospect of making long-term precipitation collections and measurements in the same region.

[42] The difference in water $\delta^{18}O$ values between Ethiopia and Kenya is likely due to differences in moisture sources. Easterly and southeasterly winds are associated with both rainy seasons in Kenya. The long rains coincide with relatively high θ_e values near the coast and indicate the Indian Ocean as a moisture source for Kenyan rainfall. $\delta^{18}O$ values from Kenya at low altitudes mimic those from Dar es Salaam and are consistent with an Indian Ocean moisture source. In contrast, westerly low-level winds coincide with precipitation events during the Kiremt rains in Ethiopia (June–September) and indicate a westerly moisture source. Moisture from this region is likely recycled by transpiration and has a higher isotopic value than waters subject strictly to Rayleigh fractionation. The Belg rains (March–April) in Ethiopia are associated with southeasterly winds. For regions of Ethiopia that receive rainfall during both the Kiremt and Belg rainy seasons, there is a seasonal oscillation between continental and Indian Ocean moisture sources.

[43] The importance of this study lies in understanding rainfall dynamics in a drought-sensitive region and in establishing a modern context with which to interpret isotopic records from the past. The isotopic divide that tracks climatic differences within eastern Africa is an expression of the Congo Air Boundary. The presence and distribution of this isotopic divide depends on topography that limits the flow of low-level air streams, the flux of

moisture from the African interior, and monsoon strength. Any changes in these parameters in past or future climate scenarios would affect the isotopic composition of waters in eastern Africa.

[44] **Acknowledgments.** We thank Chuntao Liu and Drew Peterson with their help in accessing and working with the NCEP/NCAR and TRMM data sets. We appreciate the work of Behailu Abate, Raymonde Bonnefille, Frank Brown, Seifu Kebede, Peter Kilham, Zelalam Kubsa, Jay Quade, and Sileshi Semaw, who assisted with the sample collections used in this study. We thank Lesley Chesson, Jim Ehleringer, Mike Lott, and Scott Hynek for analytical assistance and advice. We also thank Sharon Nicholson, who provided advice and perspective through several stages of this project. We appreciate the constructive comments of three anonymous reviewers. This research was supported by the grant EAR-0617010 through the National Science Foundation.

References

Adeyewa, Z. D., and K. Nakamura (2003), Validation of TRMM radar rainfall data over major climatic regions in Africa, *J. Appl. Meteorol.*, *42*(2), 331–347, doi:10.1175/1520-0450(2003)042<0331:VOTRRD>2.0.CO;2.

Anagnostou, E. N., and C. A. Morales (2002), Rainfall estimation from TOGA radar observations during LBA field campaign, *J. Geophys. Res.*, *107*(D20), 8068, doi:10.1029/2001JD000377.

Barton, C. E., D. K. Solomon, J. R. Bowman, T. E. Cerling, and M. D. Sayer (1987), Chloride budgets in transient lakes: Lakes Baringo, Naivasha, and Turkana, *Limnol. Oceanogr.*, *32*(3), 745–751.

Brubaker, K. L., D. Entekhabi, and P. S. Eagleson (1993), Estimation of continental precipitation recycling, *J. Clim.*, *6*(6), 1077–1089, doi:10.1175/1520-0442(1993)006<1077:EOCPR>2.0.CO;2.

Camberlin, P. (1997), Rainfall anomalies in the source region of the Nile and their connection with the Indian summer monsoon, *J. Clim.*, *10*(6), 1380–1392, doi:10.1175/1520-0442(1997)010<1380:RAITSR>2.0.CO;2.

Camberlin, P., and N. Philippon (2002), The east African March-May rainy season: Associated atmospheric dynamics and predictability over the 1968–97 period, *J. Clim.*, *15*, 1002–1019, doi:10.1175/1520-0442(2002)015<1002:TEAMMR>2.0.CO;2.

Cerling, T. E., J. A. Hart, and T. B. Hart (2004), Stable isotope ecology in the Ituri Forest, *Oecologia*, *138*, 5–12, doi:10.1007/s00442-003-1375-4.

Cohen, A. S., M. R. Talbot, S. M. Awramik, D. L. Dettman, and P. I. Abell (1997), Lake level and paleoenvironmental history of Lake Tanganyika, Africa, as inferred from Late Holocene and modern stromatolites, *Geol. Soc. Am. Bull.*, *109*(4), 444–460, doi:10.1130/0016-7606(1997)109<0444:LLAPHO>2.3.CO;2.

Coleman, M. L., T. J. Shepherd, J. J. Durhan, J. E. Rouse, and G. R. Moore (1982), Reduction of water with zinc for hydrogen isotope analysis, *Anal. Chem.*, *54*(6), 993–995, doi:10.1021/ac00243a035.

Conway, D. (2000), The climate and hydrology of the Upper Blue Nile River, *Geogr. J.*, *166*(1), 49–62, doi:10.1111/j.1475-4959.2000.tb00006.x.

Craig, H., and L. I. Gordon (1965), Deuterium and oxygen-18 variations in the ocean and the marine atmosphere, in *Stable Isotopes in Oceanographic Studies and Paleotemperatures*, edited E. Tongiorgi, pp. 9–130, V. Lischi, Spoleto, Italy.

Crowley, J. W., J. X. Mitrovica, R. C. Bailey, M. E. Tamisiea, and J. L. Davis (2006), Land water storage within the Congo Basin inferred from GRACE satellite gravity data, *Geophys. Res. Lett.*, *33*, L19402, doi:10.1029/2006GL027070.

Dansgaard, W. (1964), Stable isotopes in precipitation, *Tellus*, *16*, 436–468.

Dinku, T., P. Ceccato, E. Grover-Kopec, M. Lemma, S. J. Connor, and C. F. Ropelewski (2007), Validation of satellite rainfall products over East Africa's complex topography, *Int. J. Remote Sens.*, *28*(7), 1503–1526, doi:10.1080/01431160600954688.

Epstein, S., R. Buchsbaum, H. A. Lowenstam, and H. C. Urey (1953), Revised carbonate-water isotopic temperature scale, *Geol. Soc. Am. Bull.*, *64*, 1315–1326, doi:10.1130/0016-7606(1953)64[1315:RCITS]2.0.CO;2.

Fessenden, J. E., C. S. Cook, M. J. Lott, and J. R. Ehleringer (2002), Rapid ^{18}O analysis of small water and CO_2 samples using a continuous-flow isotope ratio mass spectrometer, *Rapid Commun. Mass Spectrom.*, *16*(13), 1257–1260, doi:10.1002/rcm.711.

Gamachu, D. (1977), *Aspects of Climate and Water Budget in Ethiopia*, 71 pp., Addis Ababa Univ. Press, Addis Ababa.

Gat, J. R. (1996), Oxygen and hydrogen isotopes in the hydrologic cycle, *Annu. Rev. Earth Planet. Sci.*, *24*, 225–262, doi:10.1146/annurev.earth.24.1.225.

Gat, J. R. (2000), Atmospheric water balance–The isotopic perspective, *Hydrol. Processes*, *14*(8), 1357–1369, doi:10.1002/1099-1085(20000615)14:8<1357::AID-HYP986>3.0.CO;2-7.

Gat, J. R., and E. Matsui (1991), Atmospheric water balance in the Amazon Basin: An isotopic evapotranspiration model, *J. Geophys. Res.*, *96*(D7), 13,179–13,188, doi:10.1029/91JD00054.

Gat, J. R., C. J. Bowser, and C. Kendall (1994), The contribution of evaporation from the Great Lakes to the continental atmosphere: Estimate based on stable isotope data, *Geophys. Res. Lett.*, *21*(7), 557–560, doi:10.1029/94GL00069.

Gedzelman, S. D., and R. Arnold (1994), Modeling the isotopic composition of precipitation, *J. Geophys. Res.*, *99*(D5), 10,455–10,471, doi:10.1029/93JD03518.

Gedzelman, S. D., and J. R. Lawrence (1990), The isotopic composition of precipitation from two extratropical cyclones, *Mon. Weather Rev.*, *118*(2), 495–509, doi:10.1175/1520-0493(1990)118<0495:TICOPF>2.0.CO;2.

Gonfiantini, R. (1986), Environmental isotopes in lake studies, in *Handbook of Environmental Isotope Geochemistry*, edited by P. Fritz and J. C. Fontes, pp. 113–168, Elsevier, Amsterdam.

Gonfiantini, R., M.-A. Roche, J.-C. Olivry, J.-C. Fontes, and G. M. Zuppi (2001), The altitude effect on the isotopic composition of tropical rains, *Chem. Geol.*, *181*, 147–167, doi:10.1016/S0009-2541(01)00279-0.

Gong, C., and E. Eltahir (1996), Sources of moisture for rainfall in west Africa, *Water Resour. Res.*, *32*(10), 3115–3121, doi:10.1029/96WR01940.

Griffiths, J. F. (1972), *Climates of Africa*, 604 pp., Elsevier, Amsterdam.

Hodges, K. I., and C. D. Thorncroft (1997), Distribution and statistics of African mesoscale convective weather systems based on the ISCCP Meteosat imagery, *Mon. Weather Rev.*, *125*(11), 2821–2837, doi:10.1175/1520-0493(1997)125<2821:DASOAM>2.0.CO;2.

Houze, R. A. (1993), *Cloud Dynamics*, 573 pp., Academic, San Diego, Calif.

Joseph, A., J. P. Frangi, and J. F. Aranyossy (1992), Isotope characteristics of meteoric water and groundwater in the Sahelo-Sudanese Zone, *J. Geophys. Res.*, *97*(D7), 7543–7551.

Kalnay, E., et al. (1996), The NCEP/NCAR 40-year reanalysis project, *Bull. Am. Meteorol. Soc.*, *77*(3), 437–471, doi:10.1175/1520-0477(1996)077<0437:TNYRP>2.0.CO;2.

Kendall, C., and T. B. Coplen (2001), Distribution of oxygen-18 and deuterium in river waters across the United States, *Hydrol. Processes*, *15*, 1363–1393, doi:10.1002/hyp.217.

Kistler, R., et al. (2001), The NCEP–NCAR 50-year reanalysis: Monthly means CD-ROM and documentation, *Bull. Am. Meteorol. Soc.*, *82*(2), 247–267, doi:10.1175/1520-0477(2001)082<0247:TNNYRM>2.3.CO;2.

Kozu, T., T. Kawanishi, H. Kuroiwa, M. Kojima, K. Oikawa, H. Kumagai, K. I. Okamoto, M. Okumura, H. Nakatsuka, and K. Nishikawa (2001), Development of precipitation radar onboard the Tropical Rainfall Measuring Mission (TRMM) satellite, *IEEE Trans. Geosci. Remote Sens.*, *39*(1), 102–116, doi:10.1109/36.898669.

Krishnamurti, T. N., J. Molinari, and H. L. Pan (1976), Numerical simulation of the Somali Jet, *J. Atmos. Sci.*, *33*, 2350–2362, doi:10.1175/1520-0469(1976)033<2350:NSOTSJ>2.0.CO;2.

Kummerow, C., W. Barnes, T. Kozu, J. Shiue, and J. Simpson (1998), The Tropical Rainfall Measuring Mission (TRMM) sensor package, *J. Atmos. Oceanic Technol.*, *15*, 809–817, doi:10.1175/1520-0426(1998)015<0809:TTRMMT>2.0.CO;2.

Lachniet, M. S., and W. P. Patterson (2002), Stable isotope values of Costa Rican surface waters, *J. Hydrol.*, *260*, 135–150, doi:10.1016/S0022-1694(01)00603-5.

Lawrence, J. R., and J. W. C. White (1991), The elusive climate signal in the isotopic composition of precipitation, in *Stable Isotope Geochemistry: A Tribute to Samuel Epstein*, edited by H. P. Taylor, J. R. O'Neil, and I. R. Kaplan, pp. 169–185, Geochem. Soc., San Antonio, Tex.

Lawrence, J. R., S. D. Gedzelman, D. Dexheimer, H.-K. Cho, G. D. Carrie, R. Gasparini, C. R. Anderson, K. P. Bowman, and M. I. Biggerstaff (2004), Stable isotopic composition of water vapor in the tropics, *J. Geophys. Res.*, *109*, D06115, doi:10.1029/2003JD004046.

Leroux, M. (2001), *The Meteorology and Climate of Tropical Africa*, 548 pp., Praxis, Chichester, U. K.

Levin, N. E., J. Quade, S. W. Simpson, S. Semaw, and M. J. Rogers (2004), Isotopic evidence for Plio-Pleistocene environmental change at Gona, Ethiopia, *Earth Planet. Sci. Lett.*, *219*, 93–110, doi:10.1016/S0012-821X(03)00707-6.

Liao, L., R. Meneghini, and T. Iguchi (2001), Comparisons of rain rate and reflectivity factor derived from the TRMM precipitation radar and the WSR-88D over the Melbourne, Florida, Site, *J. Atmos. Oceanic Technol.*, *18*, 1959–1974, doi:10.1175/1520-0426(2001)018<1959:CORRAR>2.0.CO;2.

Liu, C., and E. J. Zipser (2008), Diurnal cycles of precipitation, clouds, and lightning in the tropics from 9 years of TRMM observations, *Geophys. Res. Lett.*, *35*, L04819, doi:10.1029/2007GL032437.

Liu, C., E. J. Zipser, D. J. Cecil, S. W. Nesbitt, and S. Sherwood (2008), A cloud and precipitation feature database from 9 years of TRMM observations, *J. Appl. Meteorol. Climatol.*, *47*, 2712–2728, doi:10.1175/2008JAMC1890.1.

Mohamed, Y. A., H. H. G. Savenije, W. G. M. Bastiaanssen, and B. J. J. M. vandenHurk (2006), New lessons on the Sudd hydrology learned from remote sensing and climate modeling, *Hydrol. Earth Syst. Sci.*, *10*, 507–518. (Available at http://www.hydrol-earth-syst-sci.net/10/507/2006/hess-10-507-2006.html/)

Moreira, M. Z., L. D. S. L. Sternberg, L. A. Martinelli, R. L. Victoria, E. M. Barbosa, L. C. M. Bonates, and D. C. Nepstad (1997), Contribution of transpiration to forest ambient vapour based on isotopic measurements, *Global Change Biol.*, *3*, 439–450, doi:10.1046/j.1365-2486.1997.00082.x.

Negri, A. J., T. L. Bell, and L. Xu (2002), Sampling of the diurnal cycle of precipitation Using TRMM, *J. Atmos. Oceanic Technol.*, *19*, 1333–1344, doi:10.1175/1520-0426(2002)019<1333:SOTDCO>2.0.CO;2.

Nesbitt, S. W., and E. J. Zipser (2003), The diurnal cycle of rainfall and convective intensity according to three years of TRMM measurements, *J. Clim.*, *16*, 1456–1475, doi:10.1175/1520-0442(2003)016<1456:TDCORA>2.0.CO;2.

Nesbitt, S. W., E. J. Zipser, and D. J. Cecil (2000), A census of precipitation features in the tropics using TRMM: Radar, ice scattering, and lightning observations, *J. Clim.*, *13*, 4087–4106, doi:10.1175/1520-0442(2000)013<4087:ACOPFI>2.0.CO;2.

Nicholson, S. E. (1996), A review of climate dynamics and climate variability in eastern Africa, in *The Limnology, Climatology and Paleoclimatology of the East African Lakes*, edited by T. C. Johnson and E. O. Odada, pp. 25–56, Gordon and Breach, Amsterdam.

Nicholson, S. E., et al. (2003), Validation of TRMM and other rainfall estimates with a high-density gauge dataset for West Africa. Part II: Validation of TRMM rainfall products, *J. Appl. Meteorol.*, *42*, 1355–1368, doi:10.1175/1520-0450(2003)042<1355:VOTAOR>2.0.CO;2.

Poage, M. A., and C. P. Chamberlain (2001), Empirical relationships between elevation and the stable isotope composition of precipitation and surface waters: Considerations for studies of paleoelevation change, *Am. J. Sci.*, *301*(1), 1–15, doi:10.2475/ajs.301.1.1.

Risi, C., S. Bony, F. Vimeux, L. Descroix, B. Ibrahim, E. Lebreton, I. Mamadou, and B. Sultan (2008), What controls the isotopic composition of the African monsoon precipitation? Insights from event-based precipitation collected during the 2006 AMMA field campaign, *Geophys. Res. Lett.*, *35*, L24808, doi:10.1029/2008GL035920.

Rowley, D. B., and C. N. Garzione (2007), Stable isotope-based paleoaltimetry, *Annu. Rev. Earth Planet. Sci.*, *35*, 463–508, doi:10.1146/annurev.earth.35.031306.140155.

Rozanski, K., L. Araguas-Araguas, and R. Gonfiantini (1993), Isotopic patterns in modern global precipitation, in *Climate Change in Continental Isotopic Records*, *Geophys. Monogr. Ser.*, vol. 78, edited by P. K. Swart et al., pp. 1–36, AGU, Washington, D. C.

Rozanski, K., L. Araguas-Araguas, and R. Gonfiantini (1996), Isotope patterns of precipitation in the East African region, in *The Limnology, Climatology and Paleoclimatology of the East African Lakes*, edited by T. C. Johnson and E. O. Odada, pp. 79–93, Gordon and Breach, Amsterdam.

Russell, J. M., and T. C. Johnson (2006), The water balance and stable isotope hydrology of Lake Edward, Uganda-Congo, *J. Great Lakes Res.*, *32*, 77–90, doi:10.3394/0380-1330(2006)32[77:TWBASI]2.0.CO;2.

Salati, E., A. Dall'Olio, E. Matsui, and J. R. Gat (1979), Recycling of water in the Amazon Basin: An isotopic study, *Water Resour. Res.*, *15*(5), 1250–1258, doi:10.1029/WR015i005p01250.

Schumacher, C., and R. A. Houze (2006), Stratiform precipitation production over sub-Saharan Africa and the tropical East Atlantic as observed by TRMM, *Q. J. R. Meteorol. Soc.*, *132*, 2235–2255, doi:10.1256/qj.05.121.

Sharp, Z. D., V. Atudorei, and T. Durakiewicz (2001), A rapid method for determination of hydrogen and oxygen isotope ratios from water and hydrous minerals, *Rapid Commun. Mass Spectrom.*, *178*, 197–210, doi:10.1002/rcm.3382.

Slingo, J., H. Spencer, B. Hoskins, P. Berrisford, and E. Black (2005), The meteorology of the Western Indian Ocean, and the influence of the East African Highlands, *Philos. Trans. R. Soc. A*, *363*, 25–42, doi:10.1098/rsta.2004.1473.

Sonntag, C., E. Klitzsch, E. P. Löhnert, E. M. El-Shazly, K. O. Münnich, C. Junghans, U. Thorweihe, K. Weistroffer, and F. M. Swailem (1979), Palaeoclimatic information from deuterium and oxygen-18 in carbon-14-dated North Saharian groundwaters, in *Isotope Hydrology*, pp. 569–581, Int. At. Energy Agency, Vienna.

Taupin, J.-D., A. Coudrain-Ribstein, R. Gallaire, G. M. Zuppi, and A. Filly (2000), Rainfall characteristics ($\delta^{18}O$, $\delta^{2}H$, ΔT and ΔH_r) in western Africa: Regional scale and influence of irrigated areas, *J. Geophys. Res.*, *105*(D9), 11,911–11,924, doi:10.1029/1999JD901032.

Trenberth, K. E. (1999), Atmospheric moisture recycling: Role of advection and local evaporation, *J. Clim.*, *12*(5), 1368–1381, doi:10.1175/1520-0442(1999)012<1368:AMRROA>2.0.CO;2.

Victoria, R. L., L. A. Martinelli, J. Mortatti, and J. Richey (1991), Mechanisms of water recycling in the Amazon Basin: Isotopic insights, *Ambio*, *20*(8), 384–387.

Vizy, E. K., and K. H. Cook (2003), Connections between the summer east African and Indian rainfall regimes, *J. Geophys. Res.*, *108*(D16), 4510, doi:10.1029/2003JD003452.

Wilcox, E. M., and V. Ramanathan (2001), Scale dependence of the thermodynamic forcing of tropical monsoon clouds: Results from TRMM observations, *J. Clim.*, *14*(7), 1511–1524, doi:10.1175/1520-0442(2001)014<1511:SDOTTF>2.0.CO;2.

Worden, J., et al. (2007), Importance of rain evaporation and continental convection in the tropical water cycle, *Nature*, *445*, 528–532, doi:10.1038/nature05508.

Zipser, E. J., D. J. Cecil, C. Liu, S. W. Nesbitt, and D. P. Yorty (2006), Where are the most intense thunderstorms on Earth?, *Bull. Am. Meteorol. Soc.*, *87*(8), 1057–1071, doi:10.1175/BAMS-87-8-1057.

T. E. Cerling, Department of Geology and Geophysics, University of Utah, 115 South 1460 East, Room 383, Salt Lake City, UT 84112, USA. (thure.cerling@utah.edu)

N. E. Levin, Department of Earth and Planetary Sciences, Johns Hopkins University, 3400 North Charles St., Olin 301, Baltimore, MD 21218, USA. (nlevin3@jhu.edu)

E. J. Zipser, Department of Atmospheric Sciences, University of Utah, 135 South 1450 East, Room 819, Salt Lake City, UT 84112, USA. (ed.zipser@utah.edu)